Chapter 7

On the formation and decomposition of a thin NiH_x layer on Ni(111)

We have used temperature-programmed desorption in combination with high resolution electron energy loss spectroscopy to study the interaction of atomic hydrogen and deuterium with D or H-pre-covered Ni(111). Our results show a large isotopic effect when reversing the order of the isotopes used in preparing a thin nickel hydride (deuteride) layer, capped by a (nearly)-saturated surface hydrogen (deuterium) layer. Our results also show that atomic D atoms can "hammer" surface-bound H into the subsurface sites, whereas atomic H does not "hammer" surface-bound D into the subsurface sites. The large difference in collision-induced absorption cross-section for the two isotopes has various consequences. CO desorption traces and surface roughness probed using the elastically scattered intensity of an electron beam suggest that that NiH_x patches bulge upward relative to the remaining flat hydrogen or deuterium-covered Ni(111) surface. Decomposition of the NiH_x patches releases enough energy to desorb co-adsorbed CO.

7.1 Introduction

The development of metal hydrides as on-board hydrogen storage materials for mobile applications has undergone rapid development in recent years [1]. The kinetics of hydrogenating the metal hydride after its (partial) decomposition is one of several difficulties that still need to be overcome. For light metal hydrides, e.g. $NaAlH_4$, additives have been found to accelerate this process [2,3]. However, at the atomic level, the formation of a metal hydride from a pure metal and H_2, is poorly understood, let alone the action of catalysts. Although nickel hydride's gravimetric reversible hydrogen storage capacity limits its applicability for automotive applications, this material presents an interesting case, especially since the interaction of H_2 with various clean nickel surfaces is well studied. The latter is a consequence of the use of nickel as a catalyst for industrial hydrogenation reactions.

In general, metal hydrides are formed by simply exposing the metal to hydrogen gas. Hydrogen molecules dissociate at the metal surface and dissolve into the metal to form a solid solution of hydrogen atoms in the host metal lattice. This solid solution of hydrogen, commonly referred to as the α-phase of the metal-hydrogen system, exists only at low hydrogen concentrations. When a saturation level is reached, the α-phase undergoes a transition to a distinct solid hydride phase, also referred as the ß-phase. The two processes, which together constitute the total process of hydrogen uptake by the metal, are often expressed as:

$$M + \frac{1}{2} yH_2 \leftrightarrow MH_y \text{ (α-phase)}$$

$$MH_y + \frac{1}{2}(x-y)H_2 \leftrightarrow MH_x \text{ (ß-phase)}$$

Obviously, the first reaction may be separated into the dissociated adsorption of H_2 at the metal surface, and consecutive diffusion of H into the subsurface region. The reactions are reversible and their directions are determined by the pressure of hydrogen gas and the temperature of the metal. Nickel hydride is formed at 25 ºC above 6 kbar of gaseous hydrogen leading to a nearly stoichiometric hydride phase. The decomposition of nickel hydride takes place at approximately 3.4 kbar. Slightly higher values are observed for

formation and decomposition pressures at 65 ºC. Further details can be found in Ref 4 and 5.

Hydrogen dissociation on and desorption from clean low Miller index nickel surfaces, e.g. Ni(111), Ni(100) and Ni(110), have been studied in detail over the past decades. Experiments using ultrahigh vacuum (UHV) conditions and theoretical calculations have shown that the energy barrier to dissociate H_2 on Ni(111) is 46 kJ/mol, while for Ni(100) and Ni(110) it is 52 kJ/mol and 36kJ/mol respectively [6-10]. The desorption temperature for surface-bound hydrogen on Ni(111), Ni(100), and Ni(110) was observed between 320-380 K, 220-360 K, and 230-430 K respectively [8-11]. Under UHV conditions, nickel hydride can not be formed by dosing molecular H_2.

Absorption of atomic hydrogen into the subsurface sites has been studied in detail for Ni(111) [10,12-17]. Subsurface hydrogen was created by impinging atomic hydrogen from the gas phase onto the clean Ni(111) surface by Johnson *et al.*[13]. They used temperature-programmed desorption (TPD) and high resolution electron energy loss spectroscopy to detect and identify the subsurface hydrogen atoms. An additional double-peaked desorption feature appeared in TPD spectra near 185 and 215 K. An interstitial hydrogen vibration was observed near 100 meV, which compared favorably to the subsurface hydrogen vibrational mode observed with neutron scattering [18]. Other groups have observed similar TPD features, although the absolute desorption temperature for subsurface hydrogen appears to be strongly dependent on the exact procedure used to form a thin layer of nickel hydride on the nickel single crystal surface [14-16,19,20]. Subsurface hydrogen has been found to be extremely active in hydrogenation of simple hydrocarbons [10,19-21]. In addition, the deuterium isotope has been used as a titrant in experiments of bond-selectively controlled CHD_3 dissociation on Ni(111) [22].

Considering the dynamics of hydrogen absorption into subsurface sites, two mechanisms have been suggested [10]. First, collision-induced absorption is the dynamical process in which surface-bound hydrogen atoms are ‘hammered’ into subsurface sites by the impact of energetic inert gas atoms [10]. Second, in direct penetration hydrogen atoms penetrate the Ni(111) surface from the gas phase and equilibrate in a subsurface sites. While experimental evidence for the first mechanism is strong, direct absorption from the

gas phase is considerably more difficult to prove, as collision-induced absorption by impinging atomic hydrogen onto surface-bound atomic hydrogen may be mistaken for direct absorption.

Studies of hydrogen desorption where the H atoms originate from the subsurface region report inconsistent results. Early permeation experiments by van Willigen showed for polycrystalline nickel a distribution of emerging H_2 molecules that peaked strongly around the surface normal [23]. On the contrary, Wright *et al.* [15,16] found a cosine angular distribution of desorbing D_2 molecules in combined REMPI-TPD experiments where subsurface D atoms were created by implantation. In the latter studies, the authors suggest that their results indicate that D atoms resurface at vacant sites and diffuse on the surface before recombinatively desorbing as D_2. Several theoretical studies agree that this indirect reaction pathway, in which subsurface hydrogen (H_{subs}), absorbed directly below a surface-bound hydrogen atom (H_{surf}), first moves to an adjacent subsurface site before it emerges at an empty surface site and reacts to form H_2 [24,25]. However, in contrast to this indirect mechanism, Ceyer and co-workers have proposed a direct mechanism in which a hydrogen atom resurfaces from underneath a surface-bound species (e.g. CH_3 and C_2H_4) and reacts in a single step [10,21]. A theoretical study using density-functional theory (DFT) calculations has focused on H_{subs} + $CH_{3,surf}$ and finds support for such a direct reaction pathway [26]. However, other theoretical studies report that the pathway to form CH_4 in this manner is lowest when a hydrogen atom resurfaces at an empty threefold hollow site before reacting with CH_3 [25,27].

Recently, we preformed a study of the interaction of atomic H(D) with the bare Ni(111) surface (chapter 6). Our results confirm the absorption of hydrogen in subsurface sites when exposed to atomic hydrogen from the gas phase. We observed a double peak feature at 180 and 190 K in TPD spectra and our HREEL spectra show a broad feature centered at 100 meV. As a consequence of producing the nickel hydride thin layer at lower temperatures than previous studies, we also detected molecular H_2 at the nickel hydride surface that desorbed near 125 K. We have suggested that this molecular chemisorbed state results from an upward relaxation of surface nickel atoms when subsurface hydrogen atoms are present.

In this chapter, we use TPD in combination with HREELS to study the interaction of atomic hydrogen and deuterium with D or H-pre-covered Ni(111). Our results show a large isotopic effect when reversing the order of the used isotopes in preparing a thin nickel hydride (deuteride) layer, capped by a (nearly-)saturated surface hydrogen (deuterium) layer. Based on various TPD and HREELS experiments, we draw conclusions on the relative importance of various elementary reaction steps occurring when a H(D)-covered Ni(111) surface is exposed to D(H) atoms, the mechanism for consecutive recombinative desorption, and the uniformity with which NiH_x films form.

7.2 Experiment

Experiments are carried out in an UHV system, which consists of two chambers. The top chamber is equipped with an ion sputter gun, an atomic hydrogen source (H-flux, Tectra), a bakeable UHV leak valve, and a quadrupole mass spectrometer (Balzers QMS 422) used for TPD measurement and residual gas analysis. The lower chamber contains an upgraded ELS 22 high resolution electron energy loss spectrometer and a double-pass CMA Auger electron spectrometer (Staib Instruments). The top and lower chambers are separated by a gate valve. The typical base pressure of the system is less than 1×10^{-10} mbar.

The Ni(111) single crystal, cut and polished to less than 0.1º of the low Miller-index plane (Surface Preparation Laboratories, Zaandam, the Netherlands), can be heated to 1200 K by electron bombardment and cooled to 85 K. The crystal temperature is measured by a chromel-alumel thermocouple spot-welded to the edge of the crystal. The crystal is cleaned by Ar^+ sputtering, annealing at 1100 K, followed by oxidation in 10^{-7} mbar of O_2 and reduction in 10^{-6} mbar of H_2. After cleaning, the surface cleanliness is verified by AES. The hydrogen coverage is estimated from the TPD integral taken for m/e=2. We convert the integral to an absolute coverage using the integral determined after dosing $30{,}000\times10^{-6}$ mbar*s H_2 at 85 K as a reference for 1 ML. All TPD measurements were performed with a heating rate of 1.0 K/s. The HREEL spectra were recorded at 5 to 9 meV resolution (FWHM) with typical 1×10^4 cps for the scattered elastic peak.

The dosing of the atomic hydrogen is achieved by the atomic hydrogen source. A detailed description of the atomic hydrogen source is given in chapter 6. We have noted that in our experiments the atomic hydrogen beam is actually a mixture of H and H_2 (chapter 6), however to simplify, throughout the present study we refer to this mixture as the atomic hydrogen beam. During exposure of the atomic hydrogen beam, the crystal temperature is kept below 90 K.

We also performed experiments, in which H_2^+ is dosed onto the Ni(111) surface using a sputter gun. TPD spectra taken consecutively for m/e=2 show a single and broad peak at approximately 250 K in addition to the peaks resulting from associative desorption from the surface between 320 and 380 K. These spectra strongly resemble those published in previous studies using ionic implantation [12,14,15]. However, they are quite different from TPD spectra taking after dosing atomic hydrogen using our H-Flux. In the present study, we only use and compare data that employed atomic hydrogen absorption.

7.3 Results

In this chapter, our experiments start with dosing 1 ML D (H) on the Ni(111) surface by leaking D_2 (H_2) at 85 K, followed by HREELS measurements. Next, we expose this D-(H-) covered surface to impinging atomic H (D) atoms from our atomic hydrogen source below 90 K. After exposure to the atomic beam, we again dose the original molecular isotope at 85 K. This last step is necessary to refill empty sites left on the surface after exposure to the atomic hydrogen beam. Finally, we perform TPD experiments from 90 K to 500 K and monitor m/e=2, 3 and 4 with our QMS.

Figure 7.1 shows the HREEL spectra of the Ni(111) surface after forming 1 ML H_{surf} (7.1.a), or 1 ML D_{surf}(7.1.b) at 85 K from H_2 or D_2. Both spectra are taken at 10º off-specular angle using an impact energy of the primary electron beam of 9.6 eV. At this condition, hydrogen's surface vibrations can be well observed [13]. In figure 7.1.a, the spectrum exhibits two peaks at 141 meV, and 116 meV respectively. This spectrum is very similar to previously published HREEL spectra of 1ML surface hydrogen on Ni(111) and the two peaks have been assigned to the symmetric and antisymmetric stretch modes of

hydrogen atoms, respectively [13,28]. In our HREELS experiments, the same stretch modes for deuterium atoms are observed at 100 and 77 meV, as shown in figure 7.1.b.

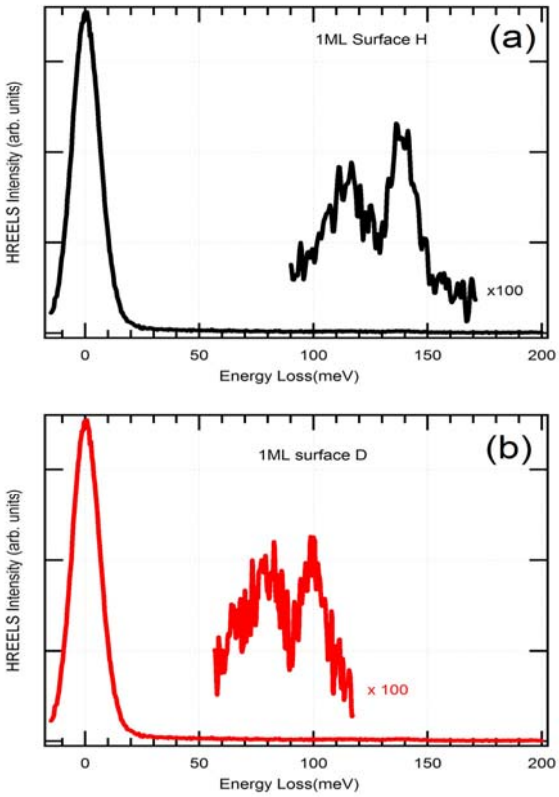

Figure 7.1 HREEL spectra of 1 ML H (a) or D (b) on Ni(111).

Figure 7.2 shows a HREEL spectrum after exposing H pre-covered Ni(111) to atomic D and finally re-dosing H_2. The spectrum shows three distinct features, a broad feature centered at 70 meV, a feature at 100 meV, and a feature at 148 meV. For comparison, figure 6.2 showed HREEL spectra for surface and subsurface H (figure 6.2 bottom trace) and surface and subsurface D (figure 6.2 top trace). The broad feature near 70 meV in figure 7.2 compares well with the 70 meV feature for subsurface deuterium in figure 6.2 (top trace). The 100 meV feature may be due to subsurface hydrogen and surface deuterium as both vibrations appear near this energy in figures 6.2 (bottom trace) and 7.1.b. The 148 meV may be assigned to surface H, although its vibrational frequency seems to have shifted

to slightly higher energy when compared to figure 7.1a. The vibrational features seem to indicate that bombarding a hydrogen-covered Ni(111) surface with D atoms leads to the formation of a thin, (mostly) hydrogen-terminated film of nickel hydride/deuteride.

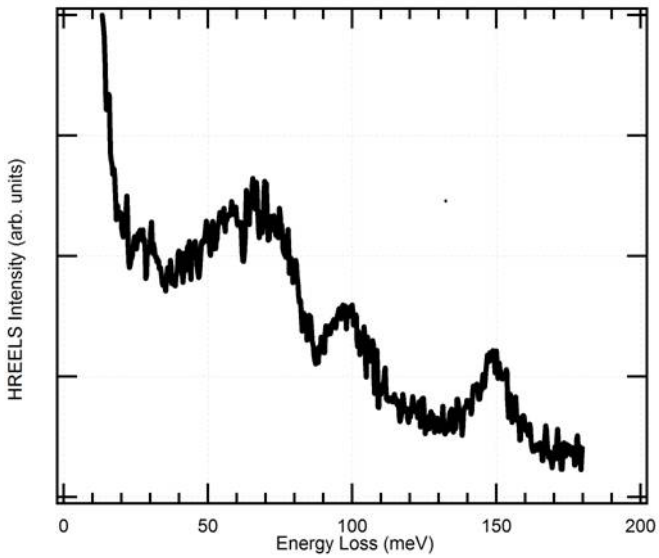

Figure 7.2 HREEL spectra taken after exposing Ni(111) to H_2, D and H_2 consecutively.

Figure 7.3 shows the variation of the HREELS elastic peak intensity after various sample treatments. The figure indicates that the intensity varies strongly after dosing molecular H_2 and atomic H or heating the crystal to different temperatures. First, the intensity increases after dosing H_2, which is expected since adsorption of hydrogen on metal surfaces increases the reflectivity of metals [29,30]. Next, the intensity decreases dramatically upon dosing atomic H to get 0.88 ML H in the subsurface region. As was mentioned in chapter 6, we suggested that the formation of this nickel hydride layer near 85 K induces surface corrugation. This corrugation is not restored after annealing the crystal at 120 and 165 K for 100 s. However, after annealing at 185 K for 100 s, half of the intensity returns. Finally, after annealing at 220 K, at which point all subsurface H has desorbed (see figures 6.1 and 7.4), the intensity returns to the value observed for (1×1)H/Ni(111). From figure 7.3 it is clear that surface corrugation is introduced when inserting hydrogen atoms

into the nickel lattice near 85 K. Surface reflectivity may be restored completely by increasing the crystal temperature temporarily to a value in between the decomposition temperature of the thin nickel hydride film and the desorption temperature of hydrogen from metallic Ni(111) surface.

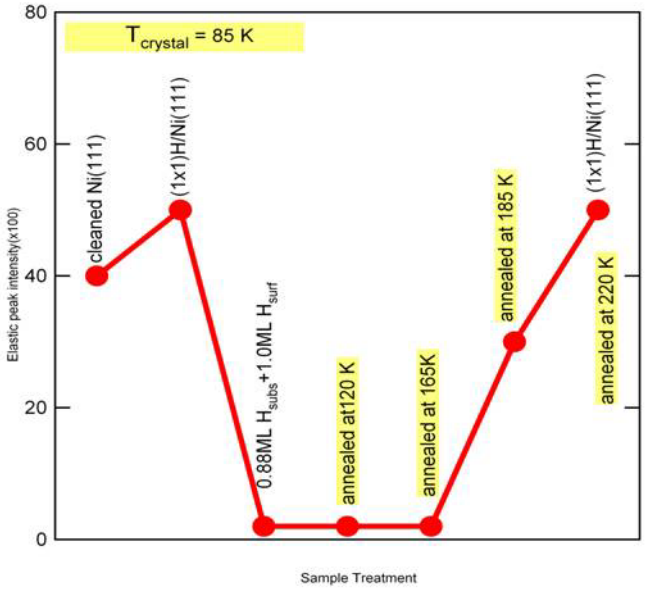

Figure 7.3 the variation of the HREELS elastic peak intensity after various sample treatments.

Six TPD spectra taken after various procedures of exposing the clean surface to atomic and molecular isotopes of hydrogen are shown in figure 7.4. There are two types of experimental variations and three different atomic doses. In figure 7.4a-c the surface was first covered with D using D_2, then exposed to atomic H, and finally re-exposed to 2×10^{-3} mbar*s D_2. In figure 7.4d-f, the isotopes were exchanged, but the order and exposures were maintained the same. The red curves represent the partial pressure of H_2 (m/e=2), the blue curves represent HD (m/e=3), and black curves represent D_2 (m/e=4). The amount of atomic exposures mentioned in figure 7.4 are rough estimates based on the atomic hydrogen source's filament temperature, H_2 (D_2) flow rates, and the distance between the atomic hydrogen source and the crystal [31]. We discuss desorption in terms of a low temperature regime (150-200 K) and a high temperature regime (300-400 K),

corresponding to decomposition of nickel hydride and associative desorption from Ni(111), respectively.

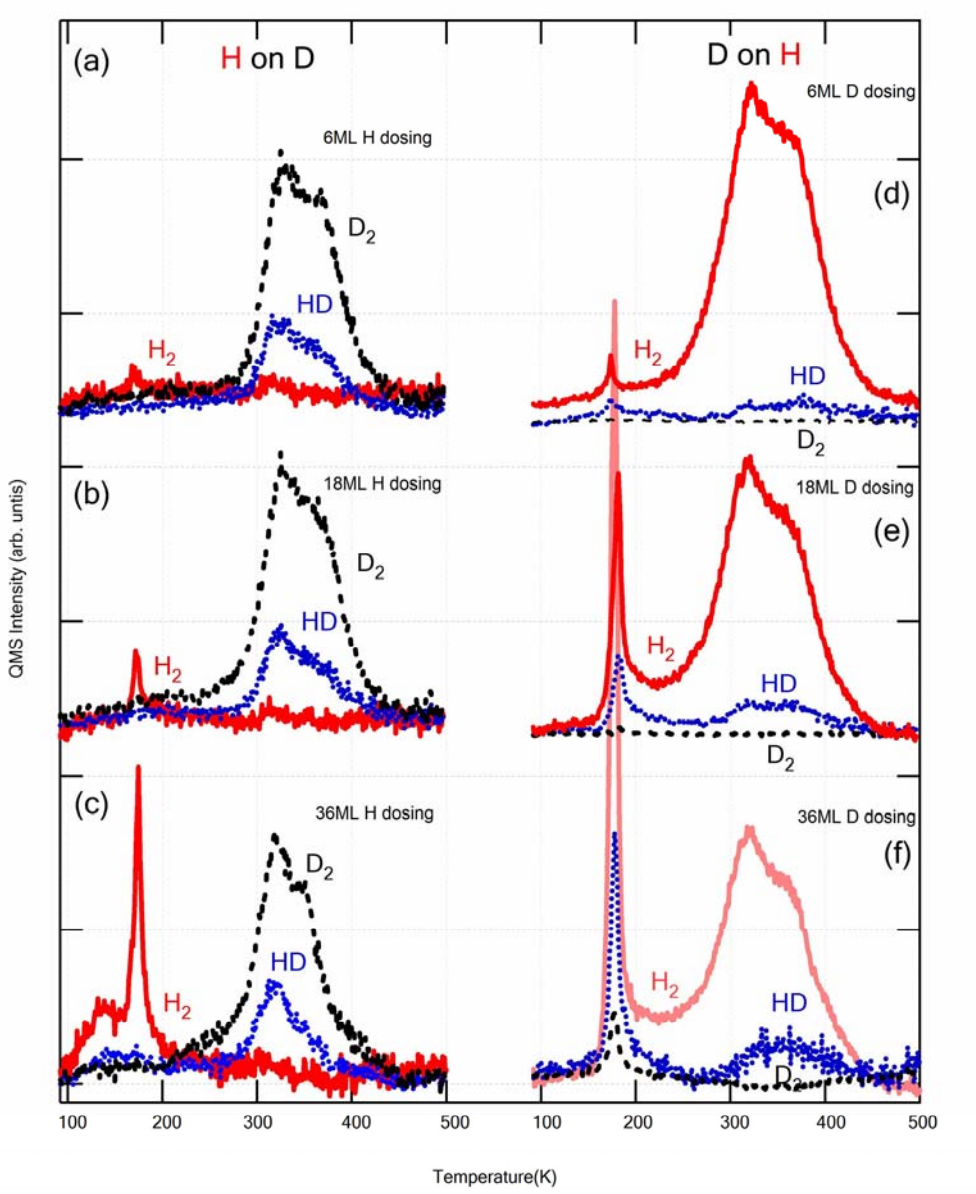

Figure 7.4 Six sets of TPD spectra of H_2, HD, and D_2 after two types of preparations. See text for detail.

Several features in figure 7.4 deserve attention. First, the rate at which desorption features in the low temperature regime appear varies with the order of employed isotopes. A surface covered initially by deuterium (7.4a-c) does not develop low temperature features nearly as fast as a hydrogen-covered surface (7.4d-f). Apparently, impinging $D_{(g)}$ on H_{surf} results in rapid build-up of interstitial species while this rate is much lower for $H_{(g)}$ impinging on D_{surf}.

Second, for $H_{(g)}$ impinging on D_{surf} (7.4a-c), only H_2 is observed in the low temperature desorption regime. The appearance of H_2 in the region of decomposition of a thin hydride film is not surprising as the surface was exposed to H atoms. However, it is noteworthy that the implanted H atoms apparently do not recombine with surface-bound D, which is plentiful judging from HD and D_2 desorption in the high temperature regime. For $D_{(g)}$ impinging on H_{surf} (7.4d-f), H_2 desorption in the low temperature regime dominates, but HD and D_2 are also observed to desorb at higher integrated D fluxes. Here, the appearance of H_2 in the low temperature regime is not obvious as the procedure to create the hydrogen terminated thin nickel hydride film involved only H_2 molecules and no H atoms.

Third, we notice in spectra where $H_{(g)}$ impinged on D_{surf}, that a significant amount of HD desorbs in the high temperature regime after the smallest integrated H flux (figure 7.4a). This amount of HD does not increase rapidly with larger H doses, while H_2 desorption in the low temperature regime increases significantly (figure 7.4b,c). Also, when comparing figure 7.4a to 7.4d, we notice that much less HD desorbs in the high temperature regime when the same amount of $D_{(g)}$ impinged on H_{surf}. In the series figure 7.4 d-f, the HD amount desorbing in the high temperature regime increases modestly with integrated D flux (figure 7.4d-f). However, even more noteworthy in these spectra is that increasing the dose of D atoms does significantly increase the amount of HD and D_2 appearing in the low temperature peak. To compare the amounts of H and D quantitatively, we have integrated the individual desorption features and, using the integral for the saturated H(D) Ni(111) surface as references, tabulated the desorbing amounts for various isotopes in table 7.1.

We note that the width of our low temperature desorption peak is much narrower than the width shown in TPD spectra for subsurface hydrogen obtained by other groups [12-14]. For example, the FWHM of the low temperature peak in figure 7.4.f is 13 K, while Ceyer

and co-workers reported approximately 50 K [13]. In chapter 6 we have suggested that this difference may be due to different preparation procedures for the thin nickel hydride layer.

Table 7.1

The list of coverages of all low temperature and high temperature peaks in figure 7.4.

dose H or D	H on D						D on H					
	Subsurface (ML)			Surface (ML)			Subsurface (ML)			Surface (ML)		
	H_2	HD	D_2	H_2	HD	D_2	H_2	HD	D_2	H_2	HD	D_2
6 ML	0.01	0	0	0	0.25	0.75	0.016	0.01	0	0.95	0.05	0
18 ML	0.025	0	0	0	0.27	0.72	0.12	0.05	0	0.9	0.1	0
36 ML	0.2	0	0	0	0.29	0.67	0.3	0.13	0.035	0.83	0.13	0.01

Finally, figure 7.5 shows two sets of TPD spectra for m/e=2 (bottom) and m/e=28 (top). In these experiments, CO is present in the chamber at low partial pressure of about ~ 5×10^{-9} mbar during exposure of the bare Ni(111) surface to atomic H below 90 K. In the H_2 desorption traces, we observe the expected desorption features in the low and high temperature regimes. In the experiment labeled “a”, the exposure to atomic hydrogen was considerably higher than in the experiment labeled “b”, leading to the equivalents of 4.5 and 1.5 ML of subsurface, respectively. In both CO TPD traces, desorption also occurs in a low and a high temperature regime. The desorption of CO in the low temperature regime strongly resembles the desorption of H_2 from the decomposition of nickel hydride thin layer and peaks at the same temperature. To our knowledge, such desorption of CO has not been previously observed. The high temperature CO desorption compares very well to previously published data [32,33] and to our own TPD studies of CO desorbing from the clean Ni(111) surface. Using the TPD trace for a saturated CO layer on Ni(111) as a

reference for the maximum coverage of 0.62 ML [33], we have quantified the total amount of CO desorbing in the experiments "a" and "b", and found that both reflect a nearly saturated CO layer. In experiment "b", 0.09 ML of CO desorbs in the low temperature regime, whereas the remaining CO desorbs in the high temperature regime. In the experiment "a", 0.15 ML CO desorbs below 200 K.

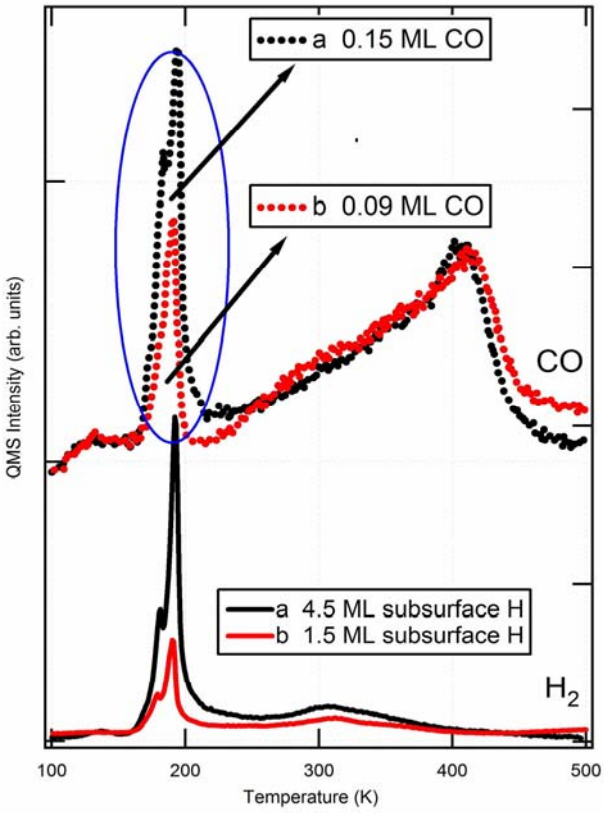

Figure 7.5 TPD spectra of m/e=2, and m/2=28, taken after impacting the bare Ni(111) surface to two different exposures of atomic H below 90 K with the presence of CO in the chamber. The numbers refer to the amounts of H and CO desorbed within the low temperature regime.

7.4 Discussions

We start the discussion with the established chemical reactions that may occur when a H(D) atom impinges on an D(H)-covered surface. The H(D) atom incident on an D(H)-covered

surface may simply reflect to the gas phase or abstract an adsorbed D_{surf}(H_{surf}) atom from the surface. This abstraction process is rreferred as the Eley-Rideal reaction:

$H_{(g)} + D_{surf} \rightarrow HD_{(g)} + *$ ("H on D",1a) and $D_{(g)} + H_{surf} \rightarrow HD_{(g)} + *$ ("D on H",1b)

This general chemical reaction may also occur through a "hot atom" mechanism [34]. A hot atom is an atom that has high translational energy. In "hot atom" mechanism, incident H(D) atoms move around on the surface as hot atoms until the excess energy is dissipated onto the surface and / or the adsorbed H(D) atoms. With the formation of $HD_{(g)}$, an empty site is created on the surface. This empty site can be filled by impacting H(D) atoms:

$H_{(g)} + * \rightarrow H_{surf}$ (2a) and $D_{(g)} + * \rightarrow D_{surf}$ (2b)

Such newly adsorbed H(D) atoms can consecutively be abstracted by the impacting H(D) atoms:

$H_{(g)} + H_{surf} \rightarrow H_{2(g)} + *$ (3a) and $D_{(g)} + D_{surf} \rightarrow D_{2(g)} + *$ (3b)

The impacting H(D) atoms may also, in parallel with the reaction 2, directly absorb into subsurface region via an empty surface site. The reaction can be expressed as:

$H_{(g)} + * \rightarrow H_{subs} + *$ (4a) and $D_{(g)} + * \rightarrow D_{subs} + *$ (4b)

Finally, impinging H(D) atoms may also lead to recombinative desorption of other atoms:

$H_{(g)} + D_{surf} + D_{surf} \rightarrow H_{surf} + D_{2(g)} + *$ (5a)

and $D_{(g)} + H_{surf} + H_{surf} \rightarrow D_{surf} + H_{2(g)} + *$ (5b)

Impacting H(D) atoms on an D(H)-covered surface can thus lead to creation of empty sites, exchange of D-H(H-D) on the surface, and absorption of H(D) in the subsurface in several parallel and consecutive reactions.

Now we consider the spectra shown in figures 7.4.d-f. As mentioned, in the experiments we only dosed molecular H_2 and atomic D. However, the H_2 TPD traces show a strong desorption feature around 180 K attributed previously to recombinative desorption of subsurface hydrogen atoms with surface-bound hydrogen atoms [13-15]. As at least half of the detected atoms in molecular H_2, HD, and D_2 observed in this temperature regime must originate from the subsurface region, subsurface H atoms must have been present after preparing the system in figures 7.4d-f. The TPD results therefore imply that exposing H-covered Ni(111) to atomic D leads to formation of H_{subs}. Apparently, in parallel with the previously mentioned reactions, reactions such as

$D_{(g)} + H_{surf} \rightarrow D_{surf} + H_{subs}$ (6) or $D_{(g)} + H_{surf} \rightarrow D_{(g)} + H_{subs}$ (7)

must also be considered.

There are two mechanisms possible for the dynamics of reactions (6) and (7). At first the surface species can be driven to a subsurface site by direct momentum transfer from an impacting atom: collision induced absorption (CIA). In addition, processes at the surface, for instance induced by hot D(H) atoms could drive atoms to a subsurface site. For instance, Ciobica *et al.* have demonstrated in DFT calculations for the H-Ru(0001) system, that a supersaturated H-overlayer is metastable and can lead to occupation of subsurface sites [35,36]. Ultimately, the supersaturated surface will relax by the ejection of molecular hydrogen to yield the saturated surface again. As we observe a very strong isotope effect in the absorption of H and D atoms and it is not clear how the relaxation of a supersaturated surface would lead to such an isotope effect, we infer that CIA is the most likely explanation of our observations.

The phenomenon of absorption through impacting species from the gas phase has been observed before for exposure of H-covered Ni(111) to various accelerated noble gas atoms from a supersonic expansion [10,37] and was referred to as CIA. The CIA process was also examined by a theoretical study, in which collisions of He, Ne, Ar, Kr, and Xe with the H-covered Ni(111) surface were simulated by molecular dynamics [38]. The simulation results show that direct collisions of noble gas atoms with adsorbed H atoms form the dominant mechanism of collision-induced absorption. The authors also suggested that there are two paths for efficient collision-induced absorption: the heavy collider path and the light collider path. The heavy collider path relies on decreasing the barrier to absorption by coupling of the impact energy to the substrate's phonons. This path dominates for collision of a heavy noble gas, e.g. Xe. The light collider path relies on transferring sufficient energy directly to an H atom so that it can overcome the energy barrier to absorb. This path dominates for collision of a light noble gas, e.g. He.

We return to considering the two types of collisions of atomic $D_{(g)}$ atoms with adsorbed H_{surf} atoms as expressed in reactions (6) and (7). Because of the small mass difference, energy transfer from impacting $D_{(g)}$ atoms to H_{surf} is even more efficient than for impacting He. Thus the light collider path is most likely to dominate this collision-induced absorption

process. In this case the required minimum energy transferred from $D_{(g)}$ to H_{surf} to absorb H_{surf} into a subsurface site equals the energy barrier for H between surface and subsurface sites. Various experimental and theoretical studies indicate that this value is close to 1 eV (100 kJ/mol) (see figure 1.1) [6,10,17,24,25]. This minimum transferred energy may be provided only by kinetic energy of $D_{(g)}$ atoms. When reaction (6) occurs, the impacting D atoms adsorb as D_{surf} after collision, so both kinetic energy of $D_{(g)}$ and potential energy released during adsorption can be transferred to H_{surf} atoms. However when reaction (7) occurs, the impacting D atoms are reflected back to gas phase after collision, so the transferred energy must only be provided by kinetic energy of $D_{(g)}$. For reaction (7), we prefer to present the simplest estimation here, in which we assume the energy transfer from $D_{(g)}$ to H_{surf} is nearly 100% and the kinetic energy of $D_{(g)}$ after collision is nearly zero. In this assumption, only the $D_{(g)}$ atoms with kinetic energy larger than 100 kJ/mol are able to "hammer" H_{surf} into subsurface sites. The velocity of such D(g) atoms should be larger than 1×10^4 m/s. According to the kinetic theory of gases, the fraction of $D_{(g)}$ atoms that have velocity larger than 1×10^4 m/s is obtained by evaluating the integral:

$$P = \int_{10^4}^{\infty} f(s)ds$$

in which $f(s)$ is the Maxwell distribution of speeds and is expressed as:

$$f(s) = 4\pi\left(\frac{M}{2\pi RT}\right)^{\frac{3}{2}} s^2 e^{-Ms^2/2RT}$$

As the cracking temperature of our H-Flux is 1800 K, such a rough estimate leads to $P \approx 0.01$ indicating that approximately 1% of $D_{(g)}$ atoms have a high enough velocity to "hammer" H_{surf} into subsurface sites. As the collision cross-section is likely small, the actual fraction of $D_{(g)}$ atoms that "hammer" H_{surf} into subsurface sites must be much smaller than 1% of the impinging flux. Comparing the fluxes in figures 7.4d-f, and the amount of H_{surf} having being "hammered" into subsurface sites in table 7.1 (0.016, 0.12, and 0.3 ML) it seems unlikely that reaction (7) dominates the creation of subsurface H atoms.

The transferred energy can also be provided by combination of kinetic energy and potential energy of $D_{(g)}$. When reaction (6) occurs, the impacting D atoms adsorb as D_{surf} after collision, so both kinetic energy of $D_{(g)}$ and potential energy released during adsorption can be transferred to H_{surf} atoms. The potential energy of a single D atom equals

the dissociation energy of ½ $D_{2(g)}$ plus the adsorption energy of a D atom on Ni(111). The dissociation energy of ½ $D_{2(g)}$ has been reported as 217 kJ/mol [39]. The adsorption energy of a H atom on Ni(111) is 46 kJ/mol. For a D atom, a minor isotope effect will change the adsorption energy. In the harmonic approximation, the difference in zero-point energies of H and D equals half of the difference between excitation frequencies, which are measured by HREELS at 141 and 100 meV for H and D, respectively, as shown in figure 7.1. Thus the zero-point energy of H is approximately 2 kJ/mol higher than D, which gives 48 kJ/mol for the adsorption energy of D. Therefore, for reaction (6), the total potential energy that may assist in CIA is 265 kJ/mol. For kinetic energy, we noted that the mean kinetic energy of $D_{(g)}$ equals $\frac{1}{2}Mc^2$, in which c is the root mean square speed of $D_{(g)}$ atoms at 1800 K. This root mean square speed is obtained by:

$$c = \left(\frac{3RT}{M} \right)^{\frac{1}{2}}$$

At 1800 K, the mean kinetic energy is 22 kJ/mol. Thus the combination of potential energy and average kinetic energy is 287 kJ/mol. This amount of energy is much larger than the energy barrier of ~100 kJ/mol for H between surface and subsurface sites. If the energy transfer efficiency from $D_{(g)}$ to H_{surf} is more than 35%, then H_{surf} can be very easily "hammered" into the subsurface site by CIA as reflected in reaction (6). A comparable study of the collision of $H_{(g)}(D_{(g)})$ with adsorbed D(H) on Pt(111) reported an energy transfer efficiency close to 50% [40]. As it does not seem unreasonable to expect a similar value for Ni(111), we conclude that reaction (6) best describes the CIA process that creates H_{subs}.

In the above discussion we have assumed that all potential energy due to the deep chemisorption well can be made available as kinetic energy to the impinging D atoms. Whether this is the case depends on the actual potential energy surface (PES). Although various theoretical studies have addressed H_{subs} + H_{surf} for Ni(111), dynamics studies performed for $H_{(g)}$ + H_{surf} on generic metal surfaces [41] and in particular on Ni(100) yield the best insight [42]. Here, attractive interaction between the gas phase H atom and H atom at the surface result in strong acceleration of the incoming H atom. Depending on the surface site for Ni(100) the acceleration is on the order of 1-2 eV. As the PES for Ni(111) is

likely comparable to that of Ni(100), we expect that CIA according to reaction (6) is likely the origin of absorbed H atoms in experiments of "D-on-H".

Based on absorption versus flux and the area of the (1×1)-H/Ni(111) unit cell we can estimate the CIA cross-section for H atoms in "D on H" experiments. As was mentioned before, table 7.1 shows that when we expose 18 and 36 ML $D_{(g)}$ on H-covered Ni(111), approximately 1% of $D_{(g)}$ atoms "hammer" H_{surf} into the subsurface sites. In combination, this value and the area of the (1×1)-H/Ni(111) unit cell yield a CIA cross-section for "D on H" of ~0.06Å^2. This is a very reasonable value considering the theoretical study of Tully *et al.* [38]. They reported a CIA cross-section of 0.04 Å^2 for impinging He atoms with 4.56 eV kinetic energy on H/Ni(111). It is noteworthy that these authors also suggest that the cross-section should increase with decreasing mass of the light collider.

For large D doses, D_2 desorption at 180 K starts appearing as shown in figure 7.4.f. This indicates that reactions:

$$D_{(g)} + * \rightarrow D_{subs} + * \quad (4b) \qquad \text{or} \qquad D_{(g)} + D_{surf} \rightarrow D_{surf} + D_{subs} \quad (8)$$

also take place when exposing the surface to atomic $D_{(g)}$ atoms. However, we can not distinguish or quantify these two reactions in the present study.

On the other hand, for "H on D", as shown in figures 7.2a-c, no desorption peaks resulting from the presence of subsurface deuterium (HD or D_2) are observed. This indicates that $H_{(g)}$ atoms do not "hammer" surface-bound D atoms into subsurface sites to a measurable extent at the conditions employed here. Therefore, the reactions

$$H_{(g)} + D_{surf} \rightarrow H_{surf} + D_{subs} \quad (9) \qquad \text{or} \qquad H_{(g)} + D_{surf} \rightarrow H_{(g)} + D_{subs} \quad (10)$$

which are the equivalent of the reactions that in the consecutive TPD experiments lead to H_2 desorption near 180 K in figures 7.4d-f, are not of significance in figures 7.4a-c. This also implies that the CIA cross-section for "H on D" must be much smaller than for "D on H". Kinetic energy transfer has been suggested to be similar for "H on D" and "D on H" resulting in similar Eley-Rideal cross-sections for "D on H" and "H on D" on Cu(111) [43]. The Eley-Rideal mechanism was proposed in 1938 by D. D. Eley and E. K. Rideal. In this mechanism, only one of the reactants adsorbs while the other reacts with it directly from the gas phase, without adsorbing. The Eley-Rideal cross section represents the surface area for this reaction to occur. Similarly, for Eley-Rideal studies on Ni(100), no large isotopic

effects were observed in any of the possible elementary reactions [42,44]. However, the authors state that they find that $D_{(g)}$ has a larger tendency to perturb H_{surf} than in the reverse case, in line with experimental observations of ER and HA reactions. Note that in this study CIA is not studied, although its occurrence is mentioned without detailed discussion [42]. Although the zero-point energy of H and D may influence the cross-sections, the energy difference is very small and should not result in significant changes [38]. We are left with two suggestions that may explain why absorption of D is not observed when using H as the 'hammer'. The first is the effect caused by coupling of the kinetic energy of impacting H(D) atoms and electronic friction prior to impact. An incoming particle towards the surface will experience an energy loss due to collision with and excitation of electrons. In a simple approximation, it can be described as a friction force acting on this particle to slow down its motion. Such friction force is also named as electronic friction. Because of a higher speed, $H_{(g)}$ experience more electronic friction prior to collision with D_{surf} than for the reverse case. $H_{(g)}$ may lose so much kinetic energy that it can not transfer enough energy to D_{surf} for CIA. The previously mentioned studies of energy loss in H(D) collision with D(H)-covered Ni(100) indicate that the average energy loss is in the order of 0.15 eV [44], which was supported by an independent theoretical study [45]. The second reason is the effect of coupling between the H_{surf}(D_{surf}) absorption dynamics and electronic friction in the substrate after collision. It has been shown that the heavier isotope D should be less affected by substrate electronic friction compared to H by Kindt *et al.* [38], resulting in more D atoms 'popping back out' after internal collisions in the subsurface cavity. Baer and coworkers include electronic friction in diffusion studies of H between surface and subsurface sites for Ni(111) and emphasize its importance in trapping the entering H atom [24]. In our experiments, such coupling effects may be the major contributor of large differences between CIA cross-sections for "H on D" and "D on H".

Upon further consideration of the H_2 formed at ~180 K in figure 7.4.a-c, we find two other noteworthy observations. First, we only observe H_2 desorption in the low temperature regime and no HD. Apparently, resurfacing H atoms do not recombine with surface-bound D even though surface-bound D atoms are the dominant species on the surface. The latter can be judged from HD and D_2 desorption in the high temperature regime. The observation

that we only find the H_2 isotope desorbing at 180 K indicates that H_{subs} formation goes in parallel with 'capping' the surface in the vicinity efficiently with H_{surf} and thus creating patches where only H is present both in the subsurface region and surface region. Recall that in our experiments we dose the original isotope molecularly after exposure to the other isotope as atoms. Had H_{subs} been created with many empty surface sites left over in the vicinity, than D_2 dissociative adsorption afterward would have resulted in HD desorption at 180 K.

The second noteworthy observation is that the absorption of H versus total H flux is initially slow but increases with exposure (see table 7.1). While dosing 6 ML H only leads to 0.01 ML H_2 desorbing at the low temperature regime, dosing 18 and 36 ML leads to 0.025 and 0.2 ML H_2 respectively. We explain the combination of this observation with the previous through a mechanism that combines reactions (1a) with consecutively (2a) and (4a). Here, an efficient CIA process of "H on H" may contribute as well. This combination of reactions yields the apparent autocatalytic effect, as 'H-isotope only reactions' can start as soon as some surface-bound D has been removed through the abstraction reaction (1a). The result of the "H-isotope only reactions" may lead to localized formation of subsurface H in patches (and thus sole H_2 desorption at 180 K) only when the rate of the consecutive reactions ((2a), (4a) and CIA of "H on H") far exceeds the rate of D-abstraction (1a). As the total amount of HD and D_2 desorbing in the high temperature regime does not increase rapidly with total H flux, this indeed seems to be the case. In addition, for the consecutive reactions, those leading to formation of empty sites are likely of less importance than those not leading to additional empty sites. For this reason it seems that reaction (2a), followed by "H on H" CIA dominates the process that induces formation of a local patch of NiH_x. In summary, as the distribution of subsurface H can not be uniform (it would have resulted in HD formation) our procedure for absorption of subsurface H in Ni(111) at 85 K must have lead to formation of patches of nickel hydride (NiH_x) in between a fairly pristine (1x1)-D/Ni(111) surface. "H on H" collision induced absorption likely played a dominant role in creation of these patches.

The results of CO experiments, as shown in figure 7.5 support our localized NiH_x hypothesis. Figure 7.5 shows that desorption of 1.5 ML subsurface H induces desorption of

0.09 ML CO at the same temperature, whereas desorption of 4.5 ML subsurface H induces desorption of 0.15 ML CO. Thus, when the amount of subsurface H increases three times, the amount of CO desorption only increases 60% in the temperature regime where subsurface H is removed. If the distribution of subsurface H were uniform, one would expect that the induced CO desorption at 180 K also increases approximately three times. However, if the formation of H_{subs} is localized as NiH_x with a capping layer of $CO_{(ads)}$, increasing of the concentration of H_{subs} (i.e. increasing x locally) does not require a proportional increase of CO desorption. Therefore, the induced CO desorption at 180 K is in agreement with our hypothesis that the formation of subsurface H is localized.

Another interesting point that we would like to note in these experiments is that the energy requirement for CO desorption is significantly larger than the energy released from a resurfacing H atom. A single resurfacing H atom has an excess energy on the order of 0.6 eV(~58 kJ/mol) to ~1 eV [15,16,24,46], while the adsorption energy of a single CO molecule at the saturation coverage and 85 K is ~1.5 eV(~145 kJ/mol) [33]. Previous studies reported that the adsorption energy of CO is not significantly affected when H is co-adsorbed on Ni(111) [47,48]. Thus, the desorption of a CO molecule at such low temperature cannot result from an individual resurfacing H atom. It seems more likely that CO desorption is due to the energy released in a phase transition of a local patch of NiH_x to (H-terminated) Ni(111). We suggest that the released energy from the phase transition leads to local heating of the surface and CO desorption.

The variation of the HREELS elastic peak intensity, as shown in figure 7.3, is also in line with our hypothesis that formation of subsurface H is localized. As was mentioned before, this variation is due to the surface corrugation at various conditions. In chapter 6, we concluded that the absorption of subsurface H in Ni(111) induces upward relaxation of surface nickel atoms. For a uniform distribution of subsurface H, one would expect that the surface is atomically smooth again when the subsurface H coverage is close to unity, e.g. 1 ML or 2 ML. However we observe that corrugation remains when the subsurface H coverage is ~ 1ML, as the HREELS elastic peak intensity drops as shown for a slightly lower subsurface concentration in figure 7.3. This observation therefore supports the suggestion regarding local formation of subsurface H in Ni(111) at 85 K. The return of the

reflectivity after annealing at 220 K, at which point all subsurface H has desorbed, indicates that in the patches of NiH_x, the Ni atoms only bulge upward. Local expansion of the nickel lattice by H absorption has also been reported in various theoretical studies [6,7,17]. Significant irreversible Ni atom transports along the surface would lead to surface roughening that would be visible through the distortion of the surface desorption features of H_2 between 300 and 400 K and a lowered final reflectivity of the elastically scattered intensity of the HREEL primary electron beam. This upward relaxation of certain patches may be difficult to detect or even invisible to LEED measurements, as the LEED image mostly reflects the structure of the (hydrogen of deuterium terminated) Ni(111) surface. For Pd(111), upward relaxation induced by absorption of H atoms has been shown using STM [49].

Finally, we note that our results also shed light on the recombinative desorption mechanism of subsurface hydrogen. In figure 7.4d-f, H_{surf} atoms are "hammered" into the subsurface sites by impacting $D_{(g)}$ atoms that stick to the surface after collision. In this case, each interstitial H atom at the octahedral subsurface site is accompanied by a surface-bound D atom right on top of it. Here, the distribution of subsurface hydrogen is expected to be fairly uniform. Now we consider the direct and indirect recombination mechanisms that may follow during the TPD ramp. In the direct recombination mechanism, a H atom directly attacks from underneath a surface-bound D atom and recombines with that D atom to form $HD_{(g)}$. This reaction is a single step and should result in HD formation in the low temperature regime. However, in figure 7.4d-f, H_2 dominates the low temperature desorption, while HD formation occurs as a minority pathway. Therefore, our data suggest that direct recombination is not dominant and the indirect recombination mechanism seems more favorable. In indirect recombination, subsurface H atoms resurface in adjacent hcp 3-fold hollow sites. For a resurfacing H atom that originally was "hammered" into subsurface by a D atom, it finds itself between two H atoms and a D atom in the adjacent fcc 3-fold hollow site. In this case, the ratio of two desorption products H_2 and HD is expected to be approximately 2:1. Table 7.1 shows that the ratios of H_2 and HD desorbing at the low temperature regime for three different $D_{(g)}$ dosing roughly reflect such a ratio. Therefore, our data supports the indirect recombination mechanism for the recombinative desorption

of subsurface hydrogen. This indirect mechanism is also favored by several experimental and theoretical studies [15, 16, 24, 25].

7.5 Conclusion

We have used TPD in combination with HREELS to study the interaction of atomic H and D with D or H-pre-covered Ni(111). Our results show that atomic D atoms can "hammer" surface-bound H into the subsurface sites, whereas atomic H does not "hammer" surface-bound D into the subsurface sites. The large difference in CIA cross-section for the two isotopes has various consequences. Experiments using "D on H" leads mostly to creation of H_{subs} through CIA, while consecutive TPD results indicate that resurfacing H atoms recombinatively desorb with surface-bound species in an indirect pathway. The CIA process dominates possible parallel reactions and has a cross-section of $0.06\,Å^2$. Experiments using "H on D" lead to formation of patches of NiH_x in an otherwise undisturbed D-covered Ni(111) surface. Here, CIA of "H on D" is absent and NiH_x patches are created by initial removal of some D_{surf} atoms, followed by more rapid H absorption processes. Here, CIA of "H on H" seems important and overtakes Eley-Rideal and other parallel reactions. CO desorption traces and surface roughness probed using the elastically scattered intensity of an electron beam suggest that that NiH_x patches bulge upward relative to the remaining flat hydrogen or deuterium-covered Ni(111) surface. Decomposition of the NiH_x patches releases enough energy to desorb co-adsorbed CO.

Finally, our observations that σ_{CIA}(D on H) >> σ_{CIA}(H on D) causes second thoughts about previously reported differences in Eley-Rideal cross-sections observed, for example, for "D on H" and "H on D" on Pt surfaces [50]. It is noteworthy that absorption of hydrogen in the first layer underneath the Pt(111) surface has recently been predicted from theoretical studies [51]. Therefore, for "D on H" the light collider CIA process may affect such studies on Pt surfaces. While for "D on H" two parallel reactions could occur (abstraction through Eley-Rideal or hot atom mechanisms and the light collider CIA), for "H on D" only abstraction reactions are likely. Thus, the Eley-Rideal cross-section for "H on D" may appear larger than for "D on H" due to a competing reaction in the latter case.

7.6 Reference

[1] L. Schlapbach, and A. Züttel, *Nature*, 2001,**414**, 353.

[2] B. Bogdanovic, and M. Schwickardi, *Appl. Phys. A,* **2001**, 72, 221.

[3] B. Sakintuna, F. L-Darkrim, and M. Hirscher, *Int. J. Hydrogen Energy,* **2007**, 32, 1121.

[4] M. V. C. Sastri, B. Viswanathan, and S. S. Murthy, *Metal Hydrides-Fundamentals and Applications*, 1998, Narosa Publishing House, New Delhi.

[5] G. Alefeld, and J. Völkl, *Hydrogen in Metals 116-Application-Oriented Properties*, 1978, Springer-Verlag, Berlin.

[6] B. Bhatia, and D. S. Sholl, *J. Chem. Phys.*, 2005, **122**, 204707.

[7] G. Kresse, and J. Hafner, *Surf. Sci.*, 2000, **459**, 287.

[8] K. Christmann, O. Schober, G. Ertl and M. Neumann, *J. Chem. Phys.*, 1974, **60**, 4528.

[9] A. Winkler, and K. D. Rendulic, *Surf. Sci.*, 1982, **118**, 19.

[10] S. T. Ceyer, *Acc. Chem. Res.,* 2001, **34**, 737.

[11] K.-Ah. Son, M. Marvikakis, and J. L. Gland, *J. Phys. Chem.*, 1995, **99**, 6270.

[12] I. Chorkendorff, J. N. Russell, and J. T. Yates, *Surf. Sci.*, 1987, **182**, 375.

[13] A. D. Johnson, K. J. Maynard, S. P. Daley, Q. Y. Yang, and S. T. Ceyer, *Phys. Rev. Lett.*, 1991, **67**, 927.

[14] H. Premm, H. Pölzl, and A. Winkler, *Surf. Sci. Lett.,* 1998, **401**, L444.

[15] S. Wright, J. F. Skelly, and A. Hodgson, *Faraday Discuss.,* 2000, **117,** 133.

[16] S. Wright, J. F. Skelly, and A. Hodgson, *Chem. Phys. Lett.*, 2002, **364,** 522.

[17] J. Greeley, and M. Mavrikakis, *Surf. Sci.*, 2003, **540**, 215.

[18] J. Eckert, C. F. Majkzrak, L. Passell, and W. B. Daniels, *Phys. Rev. B*, 1984, **29**, 3700.

[19] A. T. Capitano, K.-Ah. Son, and J. L. Gland, *J. Phys. Chem. B*. 1999, **103**, 2223.

[20] A. T. Capitano, and J. L. Gland, *Langmuir*, 1998, **14**, 1345.

[21] A. D. Johnson, S. P. Daley, A. L. Utz, and S. T. Ceyer, *Science*, 1992, **257**, 223.

[22] D. R. Killelea, V. L. Campbell, N. S. Shumann, and A.L. Utz, *Science*, 2008, **319**, 790.

[23] W. Van Willigen, *Phys. Letters,* 1968, **28A**,80.

[24] R. Baer, Y. Zeiri, and R. Kosloff, *Phys. Rev. B*, 1997, **55**, 10952.

[25] G. Henkelman, A. Arnaldsson, and H. Jónsson. *J. Chem. Phys.*, 2006, **124**, 044706.

[26] V. Ledentu, W. Dong, and P. Sautet, *J. Am. Chem. Soc.*, 2000, **122**, 1796.

[27] A. Michaelides, P. Hu, and A. Alavi, *J. Chem. Phys.*, 1999, **111**, 1343.

[28] H. Yanagita, J. Sakai, T. Aruga, N. Takagi, and M. Nishijima, *Phys. Rev. B*, 1997, **56**, 14952.

[29] L. J. Richter, B. A. Gurney, and W. Ho, *J. Chem. Phys.*, 1987, **86**, 477.

[30] G. Pauer, A. Eichler, M. Sock, M. G. Ramsey, F. Netzer, and A. Winkler, *J. Chem. Phys.*, 2003, **119**, 5253.

[31] G. Eibl, G. Lackner, and A. Winkler, *J. Vac. Sci. Technol.* A, 1998, **16**, 2979.

[32] F. P. Netzer, and T. E. Madey, *J. Chem. Phys.*, 1982, **76**, 710.

[33] G. Held, J. Schuler, W. Sklarek, and H.-P. Steinrück, *Surf. Sci.*, 1998, **398**, 154.

[34] C. T. Rettner, and D. J. Auerbach, *J. Chem. Phys.*, 1996, **104**, 2732.

[35] I. M. Ciobica, A. W. Kleyn, and R. A. Van Santen, *J. Phys. Chem.* B, 2003, **107** 164.

[36] B. Riedmüller, I. M. Ciobîcã, D. C. Papageorgopoulos, F. Frechard, B. Berenbak, A. W. Kleyn, and R. A. van Santen, *J. Chem. Phys.,* 2001, **115**, 5244.

[37] J. K. Maynard, A. D. Johnson, S. P. Daley, and S. T. Ceyer, *Faraday Discuss.,* 1991, **91,** 437.

[38] J. Kindt, and J. C. Tully, *J. Chem. Phys.*, 1999, **111**, 11060.

[39] A. Balakrishnan, and B. P. Stoicheff, J. Mol. Spectrosc, 1992, **156**, 517.

[40] J.-Y. Kim, and J. Lee, *Phys. Rev. Lett.*, 1999, **82**, 1325.

[41] B. Jackson, and D. Lemoine, *J. Chem. Phys.*, 2001, **114**, 474.

[42] Z. B. Guvenc, X. W. Sha, and B. Jackson, *J. Chem. Phys.*, 2001, **115**, 9018.

[43] D. V. Shalashilin, B. Jackson, and M. Persson, *J. Chem. Phys.*, 1999, **110**, 11038.

[44] Z. B. Guvenc, X. W. Sha, and B. Jackson, *J. Phys. Chem. B*. 2002, **106**, 8342.

[45] R. Martinazzo, S. Assoni, G. Marinoni, and G. F. Tantardini, *J. Chem. Phys.*, 2004, **120**, 8761.

[46] X. W. Sha, and B. Jackson, *Chem. Phys. Lett.*, 2002, **357,** 389.

[47] G. E. Mitchell, J. L. Gland, and J. M. White, *Surf. Sci.*, 1983, **559**, 167.

[48] W. Braun, H.-P. Steinrück, and G. Held, *Surf. Sci.*, 2005, **574**, 193.

[49] E. C. H. Sykes, L. C. F-Torres, S. U. Nanayakkara, B. A. Mantooth, R. M. Nevin, and P. S. Weiss, *PNAS*, 2005, **102**, 17907.

[50] H. Busse, M. R. Voss, D. Jerdev, B. E. Koel, and M. T. Paffett, *Surf. Sci.*, 2001, **490**, 133.

[51] P. Legare, *Surf. Sci.*, 2004, **559**, 169.